Thermonuclear Reaction Rate of ^{23}Mg(p,γ)^{24}Al

H. Herndl[1], M. Fantini[2], C. Iliadis[3,4*], P.M. Endt[5], and H. Oberhummer[1]

[1] *Institut für Kernphysik, Technische Universität Wien, Wiedner Hauptstraße 8–10, A–1040 Wien, Austria*

[2] *Dipartimento di Fisica, Universita di Trento, I-38050 Povo (Trento), Italy*

[3] *The University of North Carolina at Chapel Hill, Chapel Hill, North Carolina 27599-3255, USA*

[4] *Triangle Universities Nuclear Laboratory, Durham, North Carolina 27708-0308, USA*

[5] *R.J. Van de Graaff Laboratorium, Universiteit Utrecht, P.O. Box 80000, 3508 TA Utrecht, The Netherlands*

(March 12, 2018)

Abstract

Updated stellar rates for the reaction ^{23}Mg(p,γ)^{24}Al are calculated by using all available experimental information on ^{24}Al excitation energies. Proton and γ-ray partial widths for astrophysically important resonances are derived from shell model calculations. Correspondences of experimentally observed ^{24}Al levels with shell model states are based on application of the isobaric multiplet mass equation. Our new rates suggest that the ^{23}Mg(p,γ)^{24}Al reaction influences the nucleosynthesis in the mass A>20 region during thermonuclear runaways on massive white dwarfs.

24.50.+g, 25.40.Lw, 97.10.Cv

Typeset using REVTeX

---

*Corresponding author. E-mail: Iliadis@tunl.duke.edu

I. INTRODUCTION

Explosive stellar burning of hydrogen in the mass A>20 range is characterized by a large number of proton capture reactions and β-decays. The resulting network of nuclear processes is called the rp–process [1]. This process might be responsible for the energy production and nucleosynthesis in a variety of astrophysical sites with different temperature and density conditions. For example, in novae, typical peak temperatures range from $T_9 = 0.2 - 0.4$ [2], with T_9 the temperature in GK. For x–ray bursts and accreting black holes the rp–process could take place at very high temperatures in excess of T_9=1 [3,4]. Stellar rates of several proton capture reactions relevant for the rp–process were estimated by Wallace and Woosley [1] and by Wiescher et al. [5]. Recently, some of these rates were updated with new experimental information and improved theoretical models [6–9].

At low stellar temperatures T_9<0.1 the isotope ^{23}Mg is synthesized in the NeNa-cycle. Under such conditions the β-decay of ^{23}Mg ($T_{1/2}$=11.3 s) and the subsequent ^{23}Na(p,α) reaction convert material back into ^{20}Ne, giving rise to cycling of material in the NeNa mass range. If the stellar temperature is sufficiently high the proton capture reaction on ^{23}Mg becomes faster than the competing β-decay. In this case the reaction flow breaks out of the NeNa mass region and a whole range of heavier nuclei could be synthesized, depending on the temperature-density conditions and the duration of the astrophysical event. This scenario, for example, might be responsible for the synthesis of elements such as Si, S and Ar, which have been found to be overabundant in the ejecta of ONeMg novae [2]. Therefore, a quantitative estimate of the stellar reaction rate for ^{23}Mg(p,γ)^{24}Al is important in order to model the nucleosynthesis in the mass A>20 range. At very high temperatures above T_9=1 the ^{23}Mg(p,γ)^{24}Al reaction is of minor importance, since the isotope ^{23}Mg is bypassed via the sequence ^{21}Na(p,γ)^{22}Mg(p, γ)^{23}Al(p,γ)^{24}Si($\beta^+\nu$)^{24}Al.

The reaction rate for ^{23}Mg(p,γ)^{24}Al was previously estimated by Wallace and Woosley [1], and their calculation was based on a single resonance only. Subsequently the reaction rate calculation was improved by Wiescher et al. [5] who considered three resonances and in addition a contribution from the direct capture process. The most recent estimate was published by Kubono et al. [10]. These authors, who investigated the level structure of ^{24}Al near the proton threshold by using the ^{24}Mg(^{3}He,t)^{24}Al charge-exchange reaction, based the reaction rate estimate on their experimentally determined ^{24}Al excitation energies and spin-parity restrictions.

We present a reanalysis of the ^{23}Mg(p,γ)^{24}Al reaction rate for several reasons. First, a recent experimental study of the ^{24}Mg(^{3}He,t)^{24}Al charge-exchange reaction was published by Greenfield et al. [11]. The excitation energies of proton threshold levels in ^{24}Al measured by the two groups differ by about 30–50 keV. This difference might change the resulting reaction rates appreciably. Second, the authors of Ref. [10] conclude that the analog assignments of the two lowest-lying proton threshold states in ^{24}Al are still uncertain, resulting in large errors of the derived stellar reaction rates. Third, the proton and γ-ray partial widths of the resonances in question have never been measured. These quantities were crudely estimated in Ref. [10] by adopting 'typical' single-particle spectroscopic factors and 'average' γ-ray transition strenghts from Ref. [5].

In this work we use ^{24}Al excitation energies recommended by Ref. [12] which are based on previously published experimental results. We present additional support for the analog

assignments of the proton threshold levels in ^{24}Al. Furthermore, we calculate the proton and γ-ray partial widths of astrophysically important levels by using the nuclear shell model. In Sect. II we describe briefly the formalism for calculating stellar reaction rates. Experimental and theoretical nuclear input parameters are presented in Sect. III. Results and astrophysical implications are discussed in Sect. IV. A summary is given in Sect. V.

II. CALCULATION OF STELLAR REACTION RATES

The proton capture cross sections on sd-shell nuclei are predominantly determined by summing the contributions from isolated resonances corresponding to unbound compound nuclear states and from the nonresonant direct capture (DC) process. In the following we briefly describe the method of calculating the resonant and nonresonant (DC) contributions to the stellar reaction rates.

A. Resonant Reaction Contributions

For the reaction under consideration here the resonances are narrow and isolated. The resonant rate contribution can be calculated from resonance energies E_i and resonance strengths $\omega\gamma_i$ (both in units of MeV) [13]

$$N_A < \sigma v >_r = 1.54 \times 10^{11} (\mu T_9)^{-3/2} \sum_i (\omega\gamma)_i \exp\left(-11.605 E_i / T_9\right) \quad \text{cm}^3\text{mole}^{-1}\text{s}^{-1} \quad . \quad (1)$$

The resonance strength $\omega\gamma$ for a (p,γ) reaction is given by

$$\omega\gamma = \frac{2J+1}{2(2j_t+1)} \frac{\Gamma_p \Gamma_\gamma}{\Gamma_{\text{tot}}} \quad , \quad (2)$$

where J and j_t are the spins of the resonance and the target nucleus, respectively, and the total width Γ_{tot} is the sum of the proton partial width Γ_p and the γ-ray partial width Γ_γ.

The proton partial width Γ_p can be estimated from the single–particle spectroscopic factor S and the single–particle width Γ_{sp} of the resonance by using [14]

$$\Gamma_p = C^2 S \cdot \Gamma_{\text{sp}} \quad , \quad (3)$$

where C is the isospin Clebsch–Gordan coefficient. Spectroscopic factors S are calculated in this work by using the nuclear shell model (Sect. III). Single–particle widths Γ_{sp} are obtained from resonant scattering phase shifts generated by an appropriate folding potential (see below). In this context, the partial width Γ_{sp} is defined as the energy interval over which the resonant phase shift varies from $\pi/4$ to $3\pi/4$.

Gamma–ray partial widths for specific electromagnetic transitions are expressed in terms of reduced transition probabilities B($J_i \rightarrow J_f$;L) which contain the nuclear structure information of the states involved in the transition [15]. In the present work, the reduced transition probabilities are calculated in the framework of the nuclear shell model (Sect. III). The total γ–ray width Γ_γ of a particular resonance is given by the sum over partial γ–ray widths for transitions to all possible lower–lying nuclear states.

B. Nonresonant Reaction Contributions

The nonresonant proton capture cross section is calculated by using the direct capture (DC) model described in [16–18]. The DC cross section σ_i^{DC} for a particular transition is determined by the overlap of the scattering wave function in the entrance channel, the bound–state wave function in the exit channel and the electromagnetic multipole transition operator. Usually, only the dominant E1 transitions have to be taken into account. Wave functions are obtained by using a real folding potential given by [17,19]

$$V(R) = \lambda V_{\mathrm{F}}(R) = \lambda \int \int \rho_a(\mathbf{r}_1)\rho_A(\mathbf{r}_2) \, v_{\mathrm{eff}}\left(E, \rho_a, \rho_A, s\right) \mathrm{d}\mathbf{r}_1\mathrm{d}\mathbf{r}_2 \quad . \tag{4}$$

Here λ represents a potential strength parameter close to unity, and $s = |\mathbf{R} + \mathbf{r}_2 - \mathbf{r}_1|$, with R the separation of the centers-of-mass of the projectile and the target nucleus. The mass density distributions ρ_a and ρ_A are either derived from measured charge distributions [20] or calculated by using structure models (e.g., Hartree–Fock calculations). For the effective nucleon–nucleon interaction v_{eff} we used the DDM3Y parametrization [19]. The imaginary part of the potential has been neglected due to the small flux into other reaction channels.

The total nonresonant cross section σ_{nr} is determined by summing contributions of direct capture transitions to all bound states with single-particle spectroscopic factors S_i:

$$\sigma_{\mathrm{nr}} = \sum_i (C^2 S)_i \sigma_i^{\mathrm{DC}} \quad . \tag{5}$$

The astrophysical S–factor of a charged–particle induced reaction is defined by [13]

$$S(E) = E \exp\left(2\pi\eta\right)\sigma(E), \tag{6}$$

with η denoting the Sommerfeld parameter. If the S–factor depends only weakly on the bombarding energy the nonresonant reaction rate as a function of temperature T_9 can be expressed as

$$N_{\mathrm{A}} < \sigma v >_{\mathrm{nr}} = 7.833 \times 10^9 \left(\frac{Z_1 Z_2}{A T_9^2}\right)^{1/3} S(E_0)[\mathrm{MeVbarn}]$$

$$\times \exp\left[-4.249 \left(\frac{Z_1^2 Z_2^2 A}{T_9}\right)^{1/3}\right] \quad \mathrm{cm}^3\mathrm{mole}^{-1}\mathrm{s}^{-1} \quad , \tag{7}$$

with Z_1 and Z_2 the charges of the projectile and target, respectively, and A the reduced mass (in amu). The quantity E_0 denotes the position of the Gamow peak corresponding to the effective bombarding energy range of stellar burning.

III. EXPERIMENTAL AND THEORETICAL INPUT PARAMETERS

In this section we present a discussion of excitation energies, spectroscopic factors and γ–ray partial widths which enter in the calculation of stellar reaction rates.

Experimental excitation energies in ^{24}Al below E_x=3 MeV have been compiled by Endt [21]. The energies listed in Table 24.23 of Ref. [21] are based on ^{24}Mg(^{3}He,t) and (p,n)

reaction studies performed prior to 1990. Three recent charge–exchange reaction studies [10,11,23] also report ^{24}Al excitation energies. In the present work we use the $E_x(^{24}\text{Al})$ values compiled and evaluated by Ref. [12] which are based on experimental information. The values measured in the (p,n) study of Kiang et al. [23] have been disregarded because of the superior energy resolution and counting statistics of the (^{3}He,t) reaction studies. Our adopted excitation energies (Tables I and II) differ from the results of Kubono et al. [10] on average by about 20 keV.

Spectroscopic factors and reduced γ–ray transition strengths for the levels of astrophysical interest are calculated by using the nuclear shell model. This procedure requires the identification of experimentally observed ^{24}Al levels with calculated shell model states. For bound ^{24}Al states there is a one–to–one correspondence. However, the spins and parities of experimentally observed unbound states are not known uniquely, resulting in ambiguities for the shell model assignments. Level assignments based on a comparison of experimental and shell model excitation energies alone are not useful either, mainly due to the difficulty of the shell model in producing accurate E_x values. In this work we have used a method described in Ref. [9] to which the reader is referred for details. In brief, experimental excitation energies of ^{24}Na and ^{24}Mg states, for which the spins and parities are well–known, are used together with the isobaric multiplet mass equation (IMME) [24] in order to calculate excitation energies of ^{24}Al analog states:

$$E_x(^{24}\text{Al}) = 2E_x(^{24}\text{Mg}) - E_x(^{24}\text{Na}) + 2[c - c(\text{g.s.})] \quad . \tag{8}$$

The coefficient c is a measure for the isotensor Coulomb energy of a specific isobaric triplet and is estimated in this work by using the nuclear shell model (see below). Correspondences between experimentally observed ^{24}Al levels and shell model states are found by a) minimizing the difference between measured excitation energies and E_x values calculated from Eq. (8), and b) matching experimentally determined spin-parity restrictions with shell model quantum numbers. It can be seen from our results listed in Table I that the experimentally observed ^{24}Al states at E_x=2349 and 2534 keV most likely correspond to the 3_3^+ and 4_2^+ shell model states, respectively, in agreement with the tentative assignments of Ref. [10]. However, the experimental states at E_x=2810 and 2900 keV most likely correspond to the 2_4^+ and 3_4^+ shell model states, respectively, in contradiction with the results of Kubono et al. [10].

Shell model calculations have been performed by using the code OXBASH [22]. The isospin–nonconserving (INC) interaction of Ormand and Brown [24] is employed for the calculation of wave functions and excitation energies of T=1 triplet states in the mass A=24 system. Coefficients c in Eq. (8) are estimated from theoretical excitation energies. Shell model wave functions are used for calculating single–particle spectroscopic factors and reduced transition probabilities for M1– and E2– γ-ray decays. Resulting values of the resonance parameters are listed in Table II. It can be seen that the γ-ray partial width is much smaller than the proton partial width for all resonances considered. Therefore, the resonance strength $\omega\gamma$ depends mainly on the value of Γ_γ. Table III displays the calculated Γ_γ values for the ^{24}Al unbound states of main interest in this work together with theoretical and experimental Γ_γ values of the corresponding ^{24}Na mirror states. It can be seen that in the case of ^{24}Na the shell model γ-ray widths are in excellent agreement with the experimental values deduced from lifetime measurements.

In Table II our resonance strengths are compared to previous results [10]. For the first resonance the strengths are very similar, since the experimentally measured lifetime of the ^{24}Na mirror state was used in Ref. [10]. For the second resonance our strength $\omega\gamma$ is considerably smaller than the value of Kubono et al. [10] who adopted an 'average' γ-ray transition strength from Ref. [5]. For the third and fourth resonance the spin–parity assignments are interchanged compared to Ref. [10] (see above) which explains the discrepancy of the $\omega\gamma$ values. It should be noted that the latter two resonances have a negligible influence on the stellar reaction rates (Sect. IV).

The parameters for the direct capture (DC) contribution to the stellar reaction rates are presented in Table IV. All transitions considered are displayed together with our calculated shell model spectroscopic factors. With this information, the total astrophysical S–factor for the direct capture process into all bound states has been determined (Sect. IIb). For bombarding energies below 1 MeV the S–factor can be expressed as

$$S(E) = 22.5 - 1.1 \times 10^{-2} E + 6.9 \times 10^{-6} E^2 \quad \text{keV} \cdot \text{b}. \tag{9}$$

Our derived direct capture S-factor is about 10 % smaller than the results of Wiescher et al. [5] which were also adopted by Ref. [10].

IV. DISCUSSION

The recommended stellar rates of the ^{23}Mg(p,γ)^{24}Al reaction can be parametrized for temperatures below T_9=2 by the expression [5]

$$N_{\mathrm{A}} < \sigma v >= \sum_i A_i/T932 \exp\left(-B_i/T_9\right) + C/T923 \exp\left(-D/T913\right) \quad \text{cm}^3\text{mole}^{-1}\text{s}^{-1} \quad , \tag{10}$$

where, for example, T932 stands for $T_9^{3/2}$. The first and second term in Eq. (10) represent the contributions of all narrow resonances and the direct capture process, respectively. The parameters A_i, B_i, C and D are listed in Table V.

The various contributions to the total reaction rate are displayed in Fig. 1. The direct capture process determines the stellar rates at low temperatures of $T_9 < 0.2$. The E_R=478 keV resonance dominates the reaction rates in the range T_9=0.2–1.0. The E_R=663 keV resonance is of importance at high temperatures above T_9=1 only. The resonances at E_R=939 and 1029 keV are negligible over the whole temperature range. Our results are compared in Fig. 2 with previous work [5,10]. At stellar temperatures above T_9=1 the reaction rates of the present work are smaller than the results of Refs. [5,10] by about 70%. In the temperature range T_9=0.2-0.5 important for hydrogen burning in novae (see below) the present reaction rates deviate up to a factor of 3 from the values given in Ref. [10], and up to a factor of 2 from the results of Ref. [5]. The reaction rates for ^{23}Mg+p are therefore now based on more consistent experimental and theoretical input parameters.

Figure 3 presents temperature and density conditions for which the proton capture reaction on ^{23}Mg and the ^{23}Mg β-decay are of equal strength. The solid line is calculated by assuming a hydrogen mass fraction of X_H=0.365 [2]. Recent results of hydrodynamic studies of ONeMg novae [2] are also shown in Fig. 3. The full circles represent temperature and density conditions at the peak of the thermonuclear runaway for accretion onto white dwarfs

of different inital masses ($1.00\text{M}_\odot$, $1.25\text{M}_\odot$ and $1.35\text{M}_\odot$). Our results indicate that for white dwarfs of masses $\leq 1.25\text{M}_\odot$ the proton-capture reaction on ^{23}Mg is slower than the competing β-decay and, therefore, is of minor importance for the resulting nucleosynthesis. However, for accretion onto very massive white dwarfs ($1.35\text{M}_\odot$ model of Ref. [2]) the ^{23}Mg$(p,\gamma)^{24}$Al reaction dominates over the ^{23}Mg β-decay and will influence the nucleosynthesis in the mass A>20 range. Stellar network calculations are underway in order to investigate quantitatively the implications of our new ^{23}Mg+p reaction rates and their corresponding uncertainties. The results will be published in a forthcoming paper [26].

V. SUMMARY AND CONCLUSIONS

Improved estimates of reaction rates for ^{23}Mg$(p,\gamma)^{24}$Al are presented in this work. Resonance energies are derived from all available experimental information on ^{24}Al excitation energies. Proton and γ-ray partial widths of astrophysically important resonances are estimated from single-particle spectroscopic factors and reduced γ-ray transition probabilities, respectively, derived from shell model calculations. Correspondences of experimentally observed ^{24}Al levels with shell model states are based on application of the isobaric multiplet mass equation. In the temperature range T_9=0.2–0.5 important for the nucleosynthesis in novae the present reaction rates deviate up to a factor of three from previous results. Our new stellar rates suggest that the ^{23}Mg$(p,\gamma)^{24}$Al reaction will influence the nucleosynthesis in the mass A>20 region during thermonuclear runaways on massive white dwarfs. Quantitative predictions have to await the results of large-scale stellar network calculations.

ACKNOWLEDGMENTS

REFERENCES

[1] R.K. Wallace and S.E. Woosley, Astrophys. J. Suppl. **45**, 389 (1981).

[2] M. Politano, S. Starrfield, J.W. Truran, A. Weiss and W.M. Sparks, Astrophys. J. 448, 807 (1995).

[3] R.E. Taam, S.E. Woosley and D.Q. Lamb, Astrophys. J. 459, 271 (1996).

[4] L. Jin, W.D. Arnett and S.K. Chakrabarti, Astrophys. J. 336, 572 (1989).

[5] M. Wiescher, J. Görres, F.-K. Thielemann, and H. Ritter, Astron. Astrophys. **160**, 56 (1986).

[6] L. van Wormer, J. Görres, C. Iliadis, M. Wiescher, and F.–K. Thielemann, Astrophys. J. **432**, 326 (1994).

[7] H. Herndl, J. Görres, M. Wiescher, B.A. Brown, and L. van Wormer, Phys. Rev. C **52**, 1078 (1995).

[8] H. Schatz, A. Aprahamian, J. Görres, M. Wiescher, T. Rauscher, J.F. Rembges, F.–K. Thielemann, B. Pfeiffer, P. Möller, K.–L. Kratz, H. Herndl, B.A. Brown, and H. Rebel, Phys. Rep. , in print.

[9] C. Iliadis, P.M. Endt, N. Prantzos and W.J. Thompson, to be submitted (1998).

[10] S. Kubono, T. Kajino, and S. Kato, Nucl. Phys. A **588**, 521 (1995).

[11] M.B. Greenfield, S. Brandenburg, A.G. Drentje, P. Grasdijk, H. Riezebos, S.Y. van der Werf, A. van der Woude, M.N. Harakeh, W.A. Sterrenburg and B.A. Brown, Nucl. Phys. A **524**, 228 (1991).

[12] P.M. Endt, Nucl. Phys. A **633**, 1 (1998).

[13] C.E. Rolfs and W.S. Rodney, *Cauldrons in the Cosmos*, (The University of Chicago Press, 1988).

[14] J.P. Schiffer, Nucl. Phys. 46, 246 (1963).

[15] P.J. Brussaard and P.W.M. Glaudemans, *Shell–Model Applications in Nuclear Spectroscopy* (North–Holland, Amsterdam, 1977).

[16] K. H. Kim, M. H. Park, and B. T. Kim, Phys. Rev. C **35**, 363 (1987).

[17] H. Oberhummer and G. Staudt, in *Nuclei in the Cosmos*, edited by H. Oberhummer, (Springer–Verlag, Berlin, New York, 1991) p. 29.

[18] P. Mohr, H. Abele, R. Zwiebel, G. Staudt, H. Krauss, H. Oberhummer, A. Denker, J. W. Hammer, and G. Wolf, Phys. Rev. C **48**, 1420 (1993).

[19] A. M. Kobos, B. A. Brown, R. Lindsay, and G. R. Satchler, Nucl. Phys. A **425**, 205 (1984).

[20] H. de Vries, C. W. de Jager, and C. de Vries, At. Data Nucl. Data Tables **36**, 495 (1987).

[21] P.M. Endt, Nucl. Phys. A521, 1 (1990).

[22] B.A. Brown, A. Etchegoyen, W.D.M. Rae, and N.S. Godwin, code OXBASH, 1984 (unpublished).

[23] G.C. Kiang, H. Orihara, Y. Takahashi, A. Satoh, T. Niizeki, J. Takamatsu, M. Kabasawa, T. Kawamura, K. Furukawa, T. Nakagawa, K. Maeda, K. Ishii, K. Miura, L.L. Kiang, P.K. Teng and H. Ohnuma, Nucl. Phys. A499, 339 (1989).

[24] W.E. Ormand and B.A. Brown, Nucl. Phys. A491, 1 (1989).

[25] G. Audi and A.H. Wapstra, Nucl. Phys. A595, 409 (1995).

[26] C. Iliadis et al., to be submitted (1998).

TABLE I. Comparison of excitation energies (in MeV).

^{24}Al[a]		^{24}Na[a]		^{24}Al (IMME) [b]		^{24}Al (OXBASH) [c]	
E_x	J^π	E_x	J^π	E_x	J^π	E_x	J^π
0.0	4^+	0.0	4^+	0.0	4^+	0.0	4^+
0.426	1^+	0.472	1^+	0.441	1^+	0.448	1^+
0.510	2^+	0.563	2^+	0.450	2^+	0.580	2^+
1.107	$(1-3)^+$	1.347	1^+	1.073	1^+	1.100	1^+
1.130	$(1-3)^+$	1.341	2^+	1.069	2^+	1.126	2^+
1.275	3^+	1.345	$3(^+)$	1.283	3^+	1.374	3^+
1.559	(5^+)	1.512	$5^+(3^+)$	1.552	5^+	1.554	5^+
1.559	(2^+)	1.846	2^+	1.541	2^+	1.590	2^+
1.634	3^+	1.886	3^+	1.715	3^+	1.729	3^+
2.349	(3^+)	2.514	3^+	2.305	3^+	2.176	3^+
2.534	$(4,5)^+$	2.563	$4^+(2^+)$	2.476	4^+	2.541	4^+
2.810	2^+	2.978	$2^+(3^+)$	2.803	2^+	2.837	2^+
2.900	$(1-3)^+$	2.904	3^+	2.737	3^+	2.629	3^+

[a] Experimental values evaluated and compiled in Ref. [12].
[b] Calculated by using Eq. (8).
[c] Calculated by using the nuclear shell model.

TABLE II. Resonance parameters for the reaction ^{23}Mg(p,γ)^{24}Al.

E_x (MeV) [a]	J^π	E_R^{cm} (MeV) [b]	Γ_p (meV)	Γ_γ (meV)	$\omega\gamma$ (meV)	$\omega\gamma$ (meV) [c]
2.349±0.020	3_3^+	0.478	185	33	25	27
2.534±0.013	4_2^+	0.663	2.5×10^3	53	58	130
2.810±0.020	2_4^+	0.939	9.5×10^5	83	52	11
2.900±0.020	3_4^+	1.029	3.4×10^4	14	12	16

[a] Experimental values adopted from Ref. [12].
[b] Calculated from column 1 and $Q_{p\gamma}$=1871±4 keV [25].
[c] From Ref. [10].

TABLE III. Gamma-ray partial widths (in meV) of ^{24}Al and ^{24}Na levels.

J^π	$\Gamma_\gamma^{\mathrm{SM}}$ (^{24}Al) [a]	$\Gamma_\gamma^{\mathrm{SM}}$ (^{24}Na) [a]	$\Gamma_\gamma^{\mathrm{exp}}$ (^{24}Na) [b]
3_3^+	33	43	46 ± 14
4_2^+	53	51	> 27
2_4^+	83	93	> 27
3_4^+	14	15	13 ± 2

[a] Shell model values for the ^{24}Al – ^{24}Na mirror pair.
[b] Determined from measured lifetimes of ^{24}Na levels.

TABLE IV. Shell model spectroscopic factors of ^{24}Al bound states.

E_x(MeV)	J^π	C^2S		
		$p \to 1d_{3/2}$	$p \to 1d_{5/2}$	$p \to 2s_{1/2}$
0.000	4^+	–	0.39	–
0.426	1^+	0.0010	0.69	0.0031
0.510	2^+	0.0000	0.29	0.052
1.107	1^+	0.098	0.016	0.36
1.130	2^+	0.084	0.0001	0.30
1.275	3^+	0.024	0.0057	–
1.559	5^+	–	–	–
1.559	2^+	0.11	0.088	0.19
1.634	3^+	0.0009	0.19	–

TABLE V. Recommended parameters for the ^{23}Mg(p,γ)^{24}Al reaction rate.[a]

A_i	B_i	C	D
4.02×10^3	5.56	3.72×10^8	21.95
9.59×10^3	7.71		
8.52×10^3	10.91		
2.0×10^3	11.95		

[a] The total stellar reaction rate is given by Eq. (10).
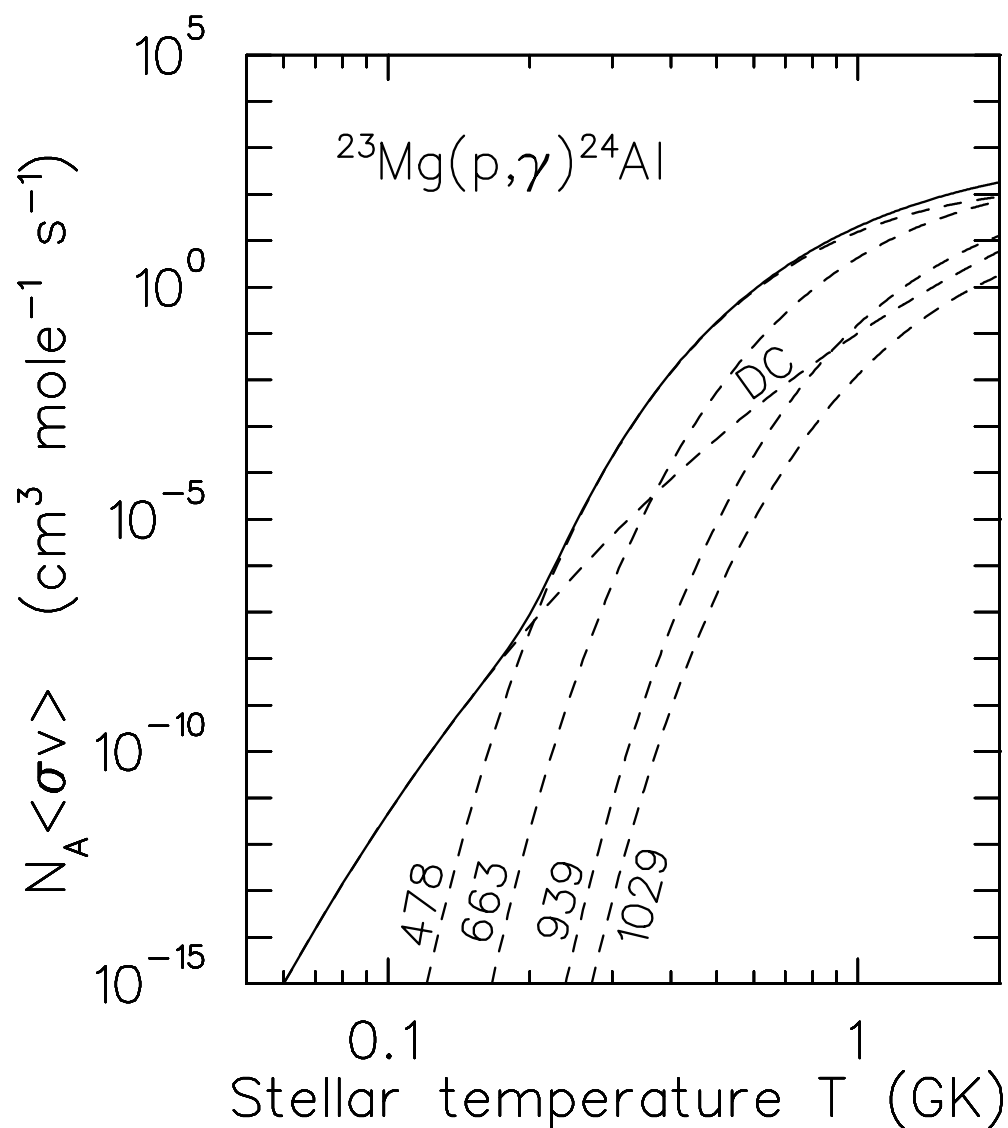
FIG. 1. Total stellar rate (solid line) and individual contributions (dashed lines) for the reaction ^{23}Mg(p,γ)^{24}Al.
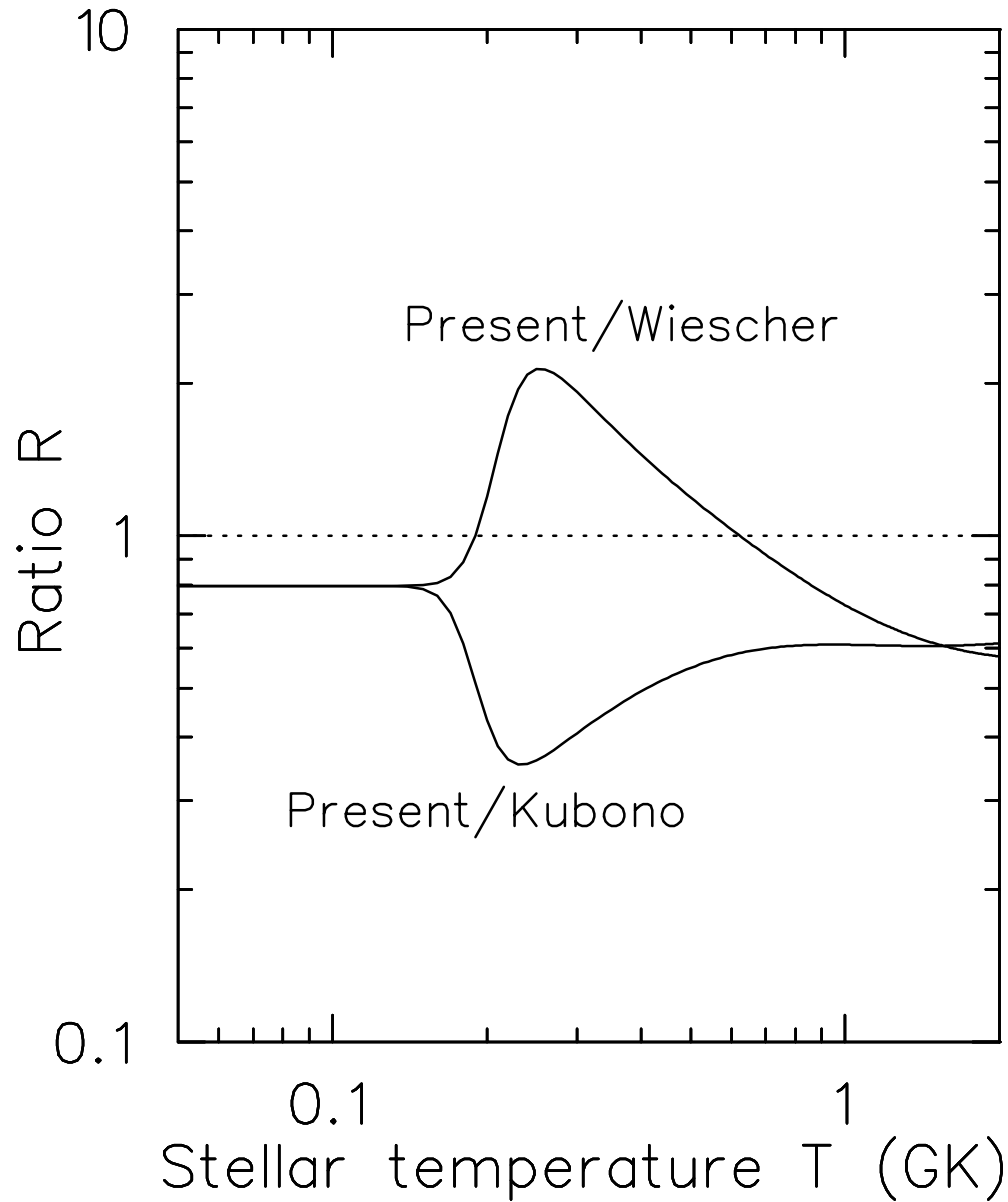
FIG. 2. Ratio of the present reaction rate to previous results of Wiescher et al. [5] and Kubono et al. [10]. The reaction rates are based on measured ^{24}Al excitation energies (see text) which are most likely Gaussian distributed.
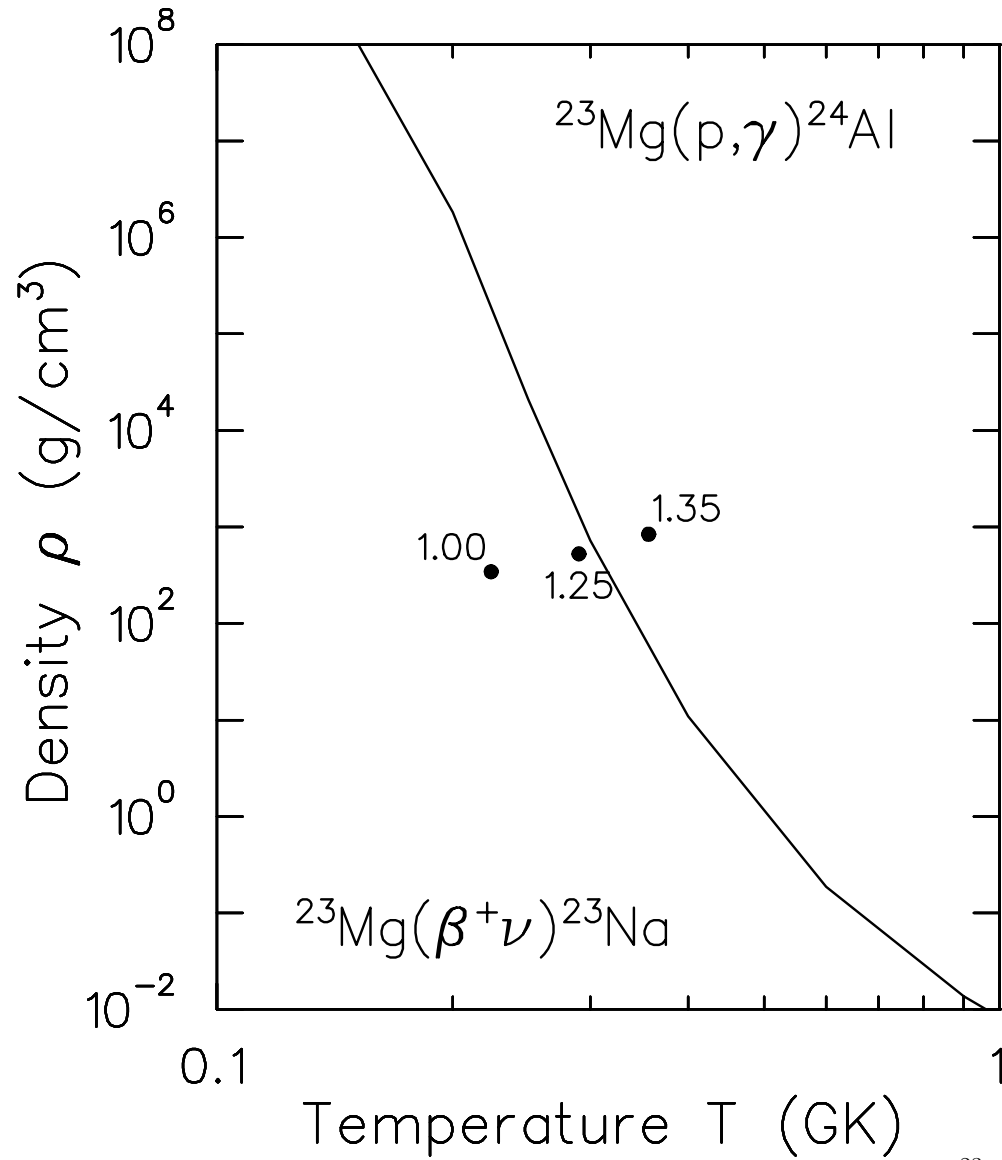
FIG. 3. Temperature-density boundary at which the proton capture reaction on ^{23}Mg and the ^{23}Mg β-decay are of equal strength, assuming a hydrogen mass fraction of $X_H=0.365$ [2]. Peak temperature and density conditions achieved in the nova models of Ref. [2] are indicated by full circles (see text).